Journal of Ovonic Research Vol. 10, No. 5, September - October 2014, p. 167 - 174

THERMAL INVESTIGATIONS OF ALUMINUM DOPED WO_3 NANOPARTICLES BY SOLVO THERMAL CUM CHEMICAL METHOD

N. PRABHU[a*], S. AGILAN[b], N. MUTHUKUMARASAMY[b], T.S.SENTHIL[c]
[a]*Department of Physics, Nandha Engineering College, Erode, India*
[b]*Department of Physics, Coimbatore Institute of Technology, Coimbatore, India*
[c]*Department of Physics, Erode Sengunthar Engineering College, Perundurai, India*

Aluminum (Al) doped Tungsten oxide (WO_3) nanoparticles have been successfully synthesized by the simple solvo thermal cum chemical method and annealed for different temperatures like room temperature (RT), 100°C and 400°C respectively. The nanoparticles have been characterized by a number of techniques as X-ray diffraction (XRD), scanning electron microscopy (SEM), Energy dispersive spectroscopy (EDX), UV-Visible spectroscopy, Fourier transform infrared spectroscopy (FTIR). The XRD results point out that all the Al doped WO_3 nanoparticles are in monoclinic form and that aluminum ions are successfully integrated into the WO_3 lattice. The presence of functional groups and the chemical bonding has been studied using FTIR spectra. Ultraviolet – Visible NIR spectral analysis were used to find its band gap (2.98-3.1eV). The SEM images used to identify the grain size of the 400°C Al doped WO_3 nanoparticles was smaller than that of room temperature (RT) Al doped WO_3 nanoparticles. It was also specific that a nanoparticle with a spherical porous structure was successfully fabricated. The EDX spectra of the Al doped WO_3 nanoparticles confirmed the presence of Al, W and O.

(Received August 29, 2014; Accepted October 8, 2014)

Keywords: Tungsten oxide, Nanoparticles, Aluminum and solvo thermal

1. Introduction

Tungsten oxide (WO_3) is one of the d° transition metal oxides, has many attractive optical, electrical, structural, and defect properties. The work on WO_3 has encouraged extensive research on a number of other transition metal oxides, and several books [1, 2] and review articles have been written on this issue [3, 4]. Among all the materials studied thus far, WO_3 has emerged as the most widely studied material, not only for chromo genies, but also for a variety of other device applications. Beyond the technology development, massive work on the physical and chemical properties of WO_3 as a prototypical material has been done that is of immense scientific interest [5]. WO_3 is a semiconductor oxide material with a band-gap of 2.6–3.0 eV [6], and it is becoming the focus of research attention due to its unique electronic properties. In particular, various WO_3 nanostructures (nanoparticles, nanoplatelets, nanorods, and nanowires) are of special interest as promising candidates for photocatalyst [6], solar cell [7] electrochromic devices [8, 9], and gas sensors [10, 11] because of their high surface area and novel properties [12].

Many physical properties of WO_3, such as piezoelectricity, electrical conductivity and defect structures, are greatly predisposed by the presence of impurities. Several dopants such as Fe, Cr, Al, Cu, Co, Mn, Mg, S, P, N etc. can lead to an increase in the surface area of the WO_3 based nano powders. Doping with other elements can greatly advance the performance of Metal oxide [13]. Among these doped metal oxide materials, aluminum (Al) doped WO_3 (AWO_3)

---

[*] Corresponding author: prabhu761984@gmail.com

nanoparticles have received significant attention [14-18]. And also have the advantage of abundant and cheap raw materials. However, the application range of Al doped WO_3 nanoparticles have been limited by the limitation of particles characteristics.

Several methods including hydrothermal [19], sol-gel [20], chemical vapor deposition (CVD) [21] and sputtering [22] have been used to prepare metal oxide nanoparticles. For efficient photo catalytic activity, nanomaterials need to be crystalline, that is, should be grown at high temperatures or at very slow rates. In general, different synthesis routes of nanostructures usually result in amorphous structures but, solvo thermal cum chemical method has the advantage in this regard as it produces self- crystallized nanostructures due to high temperature caused by joule heating. Moreover, compared with other techniques, solvo thermal cum chemical method is an attractive method because of simplicity of experimental set up, lack of need for complicated equipments, low impurity, less production steps leading to a high-throughput and cost-effective procedure to generate a high yield of nanoparticles. Also the plainness of this method allows scaling up for mass production.

The aim of the present study is to synthesize the aluminum (Al) doped tungsten oxide (WO_3) nanoparticles by simple solvo thermal cum chemical method. The prepared Al doped nano particles are annealed by different temperatures like room temperature, 100°C and 400°C respectively. And the doped nano particles are followed by structural characterizations using X-ray diffraction (XRD), scanning electron microscopy (SEM) and energy dispersive x-ray spectroscopy (EDS) and optical characterizations using UV-Visible spectroscopy and Fourier transform infrared spectroscopy (FTIR).

2. Experimental

Tungsten chloride (Sigma Aldrich 99.99%) and Cyclohexanol were used as a precursor. 40 mg of Tungsten chloride was slowly dissolved in 15 ml of Cyclohexanol to obtain a consistent solution with the help of magnetic stirrer. Then the solution was centrifuged and washed with distilled water until to reach neutral pH of the solution. After the centrifuge, the solution was subjected to slow evaporation to remove the excess solvent present in the solution at room temperature. After evaporation we got WO_3 nanoparticles. To prepare Aluminum (Al) doped WO_3 nanoparticles, we used the paste preparation method. In paste preparation method, the paste was produced by mixing of 5.0 g of Al anatase powders and 15 g of WO_3 nanoparticles with a mixture consisting of 15.0 g of α- terpineol, 2 g of cellulose, and 25 ml of ethanol, which was solicited for 60 hrs at 1200 Wcm^{-2}. By using the prepared paste thin films were prepared by coating the paste on a FTO conducting glass plate (Hartford FTO, ~30Ω cm^{-2}, 80% transmittance in visible region) using the doctor blade technique. The Al doped WO_3 nanoparticles are prepared at different temperature like room temperature, 100°C and 400°C respectively.

X-ray diffraction method using CuKα radiation has been used to study the structure of the synthesized nanoparticles. This study was carried out by employing a Brukker Axs D8 Advance X-ray differactometer with CuKα (λ=1.5406) radiation using a tube voltage and current of 40kv and 30mA respectively. The sample was scanned from 10°-80°in 2θ with step size of 0.5° 2θ and scan speed of 0.5° 2θ per second. Surface morphology of the synthesized nanoparticles was studied using scanning electron microscopy (SEM; Philips XL40), and the atomic compositions of the nanoparticles was measured by energy dispersive X-ray analyses (EDXA; Inca, oxford instruments) operated at 120 kV. The FTIR spectrum was recorded using pelletation method in the range 400 to 4000 cm-1using a Shimandzu FTIR spectrometer. The UV-Vis-NIR spectrum of the synthesized nanoparticles was recorded in the range 200-800nm using a Cary 5000(1.09 versions) with a scanning rate of 600nm/min.

3. Results and Discussion

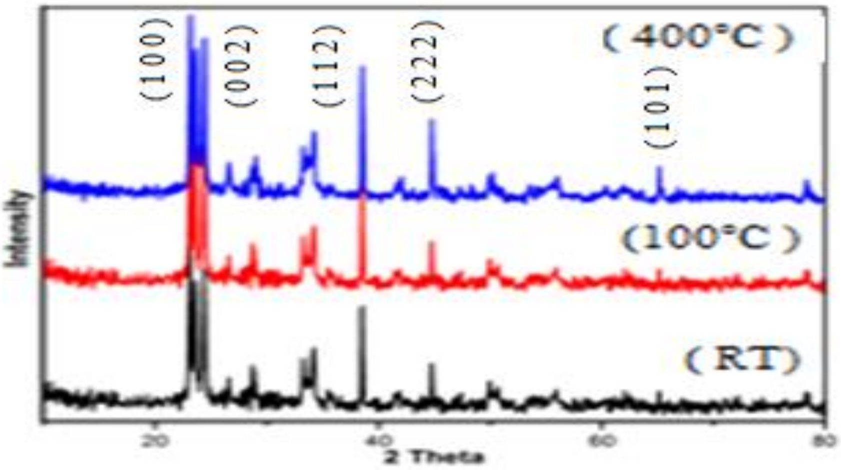

Fig. 1. X-ray diffraction pattern of Al doped WO_3 nanoparticles annealed at Room temperature (RT), 100°C and 400°C

The XRD pattern of Aluminum (Al) doped WO_3 nanoparticles with different temperatures like Room temperature (RT), 100°C and 400°C as shown in Fig. 1. All annealed Al doped WO_3 nanoparticles displayed a monoclinic, polycrystalline WO_3 structure with a main peak at 24.4Θ consequent to the (1 0 0) plane. The XRD patterns for the Al doped WO_3 samples were found to be the same as those for the room temperature, suggesting that the aluminum ions were well integrated into the WO_3 lattice. No additional peaks were detected even for 400°C, indicating that the temperature did not change the crystalline structure of the WO_3 nanoparticles. However, the intensity of the main WO_3 peaks decreased as the temperature increased, suggested that the increasing temperature may manipulate the crystalline at which WO_3 changes from amorphous to crystalline state. The line augmentation of the peak is related to the size of the monoclinic crystalline phase. The average crystallite size D, of each sample can be calculated using the Scherrer equation [23],

$$D = K \lambda / \mathrm{FWHM} \cos \theta$$

Where K is the shape factor of the average crystallite, λ is the wavelength in nanometer, FWHM is the full width at half maximum in radians, and θ is the peak position. The crystallite size of room temperature based on the (1 1 2) peak was found to be 28.7 nm. The crystallite size decreased with increasing temperature. The crystallite size was reduced to 18.2 nm under 400°C. This is because of the increasing temperature, the atomic sites enhanced the intergranular cohesion and induced lattice eccentric. Therefore, the direct relation between particles was inhibited, and crystal growth was slowed down. However, SEM measurements indicated that the particle size was much better. This is due to the agglomeration of the particles with insignificant crystal growth.

Fig. 2 shows the typical FTIR spectra of a representative Al doped WO_3 nanoparticles at 400°C with thickness of ~52 nm. One may scrutinize the subsistence of distinctive characteristic absorption peak at 825 cm^{-1} for Al doped WO_3 nanoparticles stretching modes. The peak at ~ 1641 cm^{-1} may be endorsed to aromatic C=C stretching mode. The band at 2728 cm^{-1} is the C-O stretching frequencies whereas the peak at ~2769 cm^{-1} is due to C=O bond. The broad absorption in ~2899 cm is assigned to the existence of hydroxyl groups on the surface of the samples and the absorption in ~2480 cm^{-1} is because of the existence of CO_2 molecules in air.

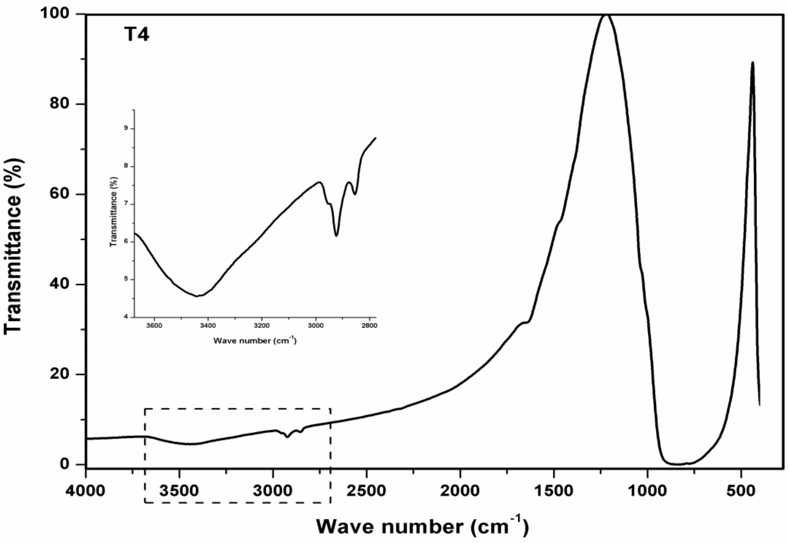

Fig. 2. The typical FTIR spectra of Al doped WO_3 nanoparticles at 400°C.

The band ~ 3400 cm $^{-1}$ is due to O-H species in the particles and those at 3200- 3600 cm $^{-1}$ are due to C-H stretching frequencies. No significant stretch mode of an N–H bond was observed, indicating that there are no physically absorbed NH_3 on the nanoparticles surface of the samples. But a lower frequency peak of low intensity at ~ 756 cm^{-1} related to Al doped WO_3 stretching modes was observed in the present spectra.

Fig. 3 shows the optical absorption spectra for Al doped WO_3 nanoparticles at different temperatures like room temperature, 100°C and 400°C respectively in the wavelength range 300 to 900 nm. It is projected that the increasing temperature of Al doped WO_3 nanoparticles will show evidence of surface Plasmon resonance and also will show a sudden concentrated absorption layer in the visible region from 550 – 900 nm. But the absence of such absorption is a clear suggestion of the acceptable entry of increasing temperature of the lattice of Al doped WO_3 nanoparticles. The quantum size shift could also be the reason for the absence of exciting peak (760 nm) and the consequent UV shift of the absorption spectra of Al doped WO_3 nanoparticles.

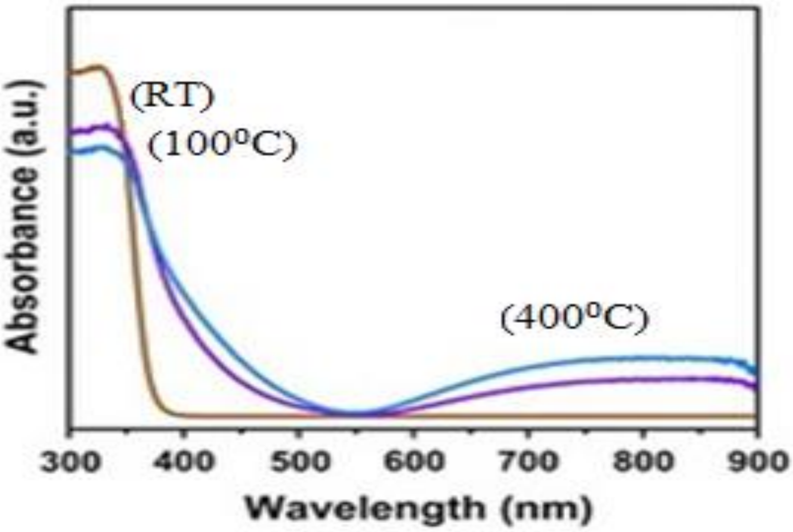

Fig. 3. UV studies for Al doped WO_3 nanoparticles at different temperatures

The optical energy gap calculated using the formula, E = hν, h is Planck's constant; ν is the photon frequency of radiation. It is found to be around for 2.98 eV for the room temperature Al doped WO_3 nanoparticles. Similarly, the band gap value of 100°C and 400°C Al doped WO_3 nanoparticles is found to be 3.04 and 3.1 eV which is higher than the band gap of room temperature Al doped WO_3 nanoparticles. The increase in band gap may be due to the quantum imprisonment result of increasing temperature.

Table 1. Variation in crystallite size and energy band gap with increasing temperature

Temperature	Crystal size (nm)	Band gap (eV)
Room temperature	28.7	2.98
100°C	23.1	3.04
400°C	18.3	3.1

The scanning electron microscope (SEM) images of the Al doped WO_3 nano particles prepared at different temperatures are shown in Fig. 4. (a), 2 (b), and 2 (c) .

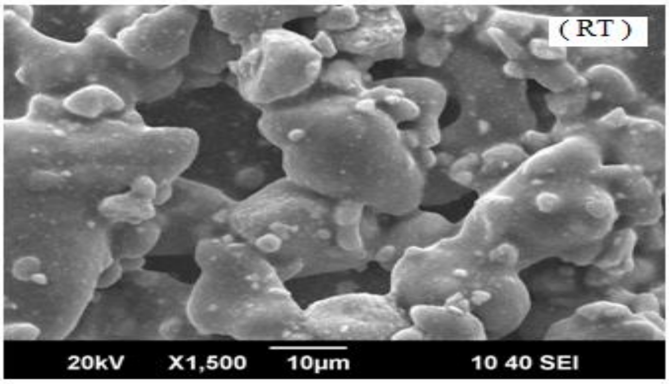

Fig. 4. (a). SEM image of Al doped WO_3 nano particles at room temperature (RT).

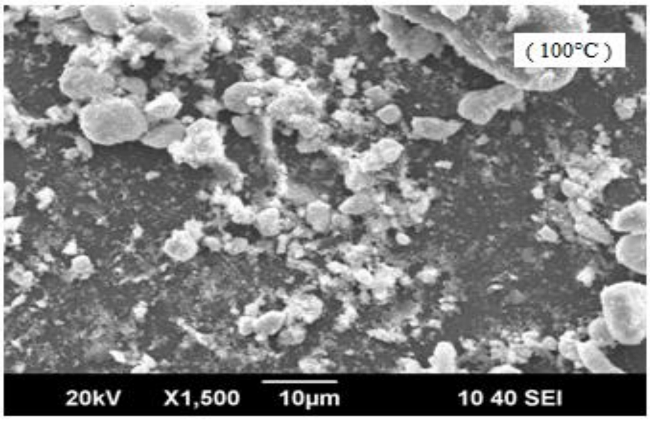

Fig. 4. (b) SEM image of Al doped WO_3 nano particles at 100°C.

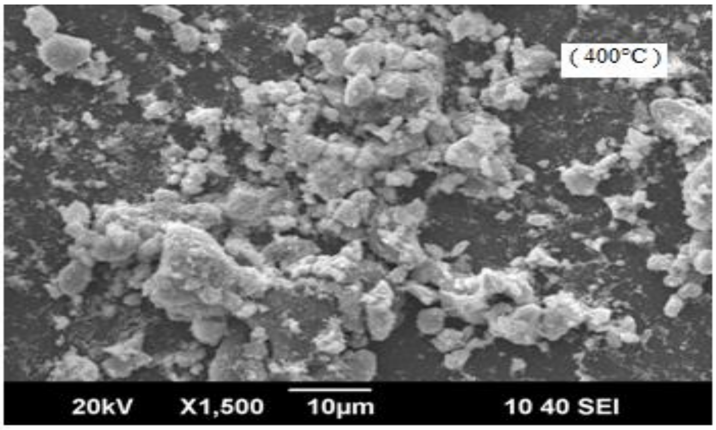

Fig. 4. (c) SEM image of Al doped WO_3 nano particles at 400°C.

Fig. 4(a), 2(b), and 2(c) presents SEM images of Al doped WO_3 nanoparticles annealed at different temperatures like room temperature (RT), 100°C and 400°C. For room temperature (RT) of Al doped WO_3 nanoparticles with a diameter of 10nm and a uniform array were observed. The spherical particles suggested that the organic compounds used in the synthesis were effectively eliminated during the annealing process. The morphology of 400°C Al doped WO_3 nanoparticles were different from that of room temperature (RT) Al doped nanoparticles. Comparing 400°C Al doped WO_3 nanoparticles with room temperature (RT) Al doped nanoparticles (Fig. 4. (c) & Fig. 4 (a)) verified that the increasing temperature presents to the agglomeration and grain growth of the Al doped WO_3 particles, leading to a rough particle surface. The grain size of the 400°C Al doped WO_3 nanoparticles was smaller than that of room temperature (RT) Al doped WO_3 nanoparticles. It was also definite that a film with a spherical porous structure was successfully fabricated. The porosity of the film is a key factor because a large surface-to-volume ratio means an increase of dye absorption, which then facilitates the photocurrent enhancement [24].

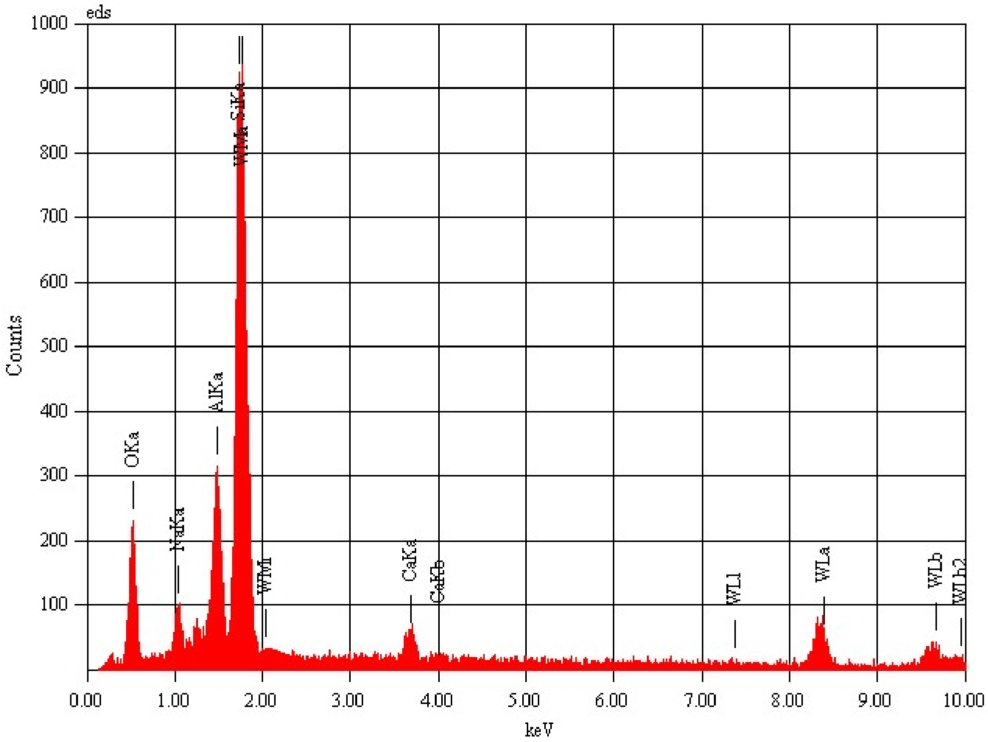

Fig. 5. EDX image of Al doped WO_3 nano particles at 400°C.

The chemical composition and concentration of the aluminum doping were investigated by energy-dispersive X-ray analysis (EDX) as well as by solvo thermal cum chemical method (Fig.5.). The EDX spectra of the Al doped WO_3 nanoparticles confirmed the presence of Al, W and O. According to EDX, Al/W ratios of different temperatures were obtained with a formal Al doped nanoparticles provided in the combination of preliminary materials. Although Al^{3+} is integrated and the real ratio correlates with the formal one, a significant percentage of the Al^{3+} clearly remains in solution so that the real doping of the solid nanomaterials is lower than expected.

4. Conclusion

This article has described the preparation of Al doped WO_3 nanoparticles annealed at different temperatures like room temperature (RT), 100°C and 400°C by a solvo thermal cum chemical method, using Tungsten chloride (Sigma Aldrich 99.99%), Cyclohexanol and Al anatase as early materials. The XRD results indicate that all the Al doped WO_3 nanoparticles are in monoclinic form and that aluminum ions are successfully incorporated into the WO_3 lattice. The presence of functional groups and the chemical bonding has been calculated using FTIR spectra. Ultraviolet – Visible NIR spectral analysis were used to find its band gap (2.98-3.1eV). The SEM images used to identify the grain size of the 400°C Al doped WO_3 nanoparticles was smaller than that of room temperature (RT) Al doped WO_3 nanoparticles. It was also specific that a film with a spherical porous structure was successfully fabricated. The EDX spectra of the Al doped WO_3 nanoparticles confirmed the presence of Al, W and O.

References

[1] C.G. Granqvist, Handbook of Inorganic Electrochromic Materials, Elsevier, Amsterdam, (1995).
[2] P.M.S. Monk, R.J. Mortimer, D.R. Rosseinsky, Electrochromism: Fundamentals and Applications, VCH, Weinheim, (1995).
[3] K. Bange, Sol. Energy Mater. Sol. Cells **58**, 1 (1999).
[4] C.G. Granqvist, Sol. Energy Mater. Sol. Cells **60,** 201 (2000)
[5] S. K. Deb, Sol. Energy Mater. Sol. Cells **92,** 245 **(**2008).
[6] F.G. Wang, C. Di Valentin, G. Pacchioni, Chem. Cat. Chem. **4,** 476 (2012).
[7] H. Zheng, Y. Tachibana, K.K Zadeh, Langumuir, **26**, 19148 (2010).
[8] S.J. Yoo, Y.H. Jung, J.W. Lim, H.G. Choi, D.K. Kim, Y.E. Sung, Sol. Energy Mater. Sol. Cells **92,** 179 (2008)
[9] H.S. Shim, J.W. Kim, Y.E. Sung, W.B. Kim, Sol. Energy Mater. Sol. Cells, **93,** 2062 (2009).
[10] J.L. Solis, S. Saukko, L. Kish, C.G. Granqvist, V. Lantto, Thin Solid Films **391,** 255 (2001) .
[11] X.L. Li, T.J. Lou, X.M. Sun, Y.D. Li, Inorg. Chem. **43,** 5442 (2004).
[12] J.H. Ha, P. Muralidharan, D.K. Kim, J. Alloys Comp. **475,** 446 (2009).
[13] S.J Oh ,M.N. Jung, S.Y Ha ,S.G. Choi ,J.J. Kim, K. Kobayashi , S.T. Lee ,H.C. Lee , Cho , T.Yao, J.H. Chang , Physica E , **41**, 31 (2008).
[14] E. Bacaksiz , S. Aksu , S. Yılmaz ,M. Parlak , M. Altunbaş , Thin Solid Films, **518** ,4076 (2010).
[15] Y.S. Kim, W.P. Tai, Applied Surface Science, **253**, 4911 (2007).
[16] R. Chandramohan, T.A. Vijayan, S. Arumugam ,H.B. Ramalingam, V. Dhanasekaran, K. Sundaram T.Mahalingam, Mater. Sci. Eng. B, **176**, 152 (2011).
[17] L. Dghoughi, F. Ouachtari, M.Addou, B. Elidrissi, H. Erguig, A. Rmili, A. Bouaoud, Physica B, **405**, 2277 (2010).
[18] E.L. Papadopoulou ,M. Varda ,A. Kouroupis-Agalou ,M. Androulidaki ,E. Chikoidze, P. Galtier, G. Huyberechts, A. Aperathitis, Thin Solid Films, **516**, 8141 (2008).
[19] M. N. Tahir, L. Gorgishvili, J. Li, T. Gorelik, U. Kolb, L. Nasdala, W. Tremel, Solid State Sci. **9** , 1105 (2007).

[20] A.K. Srivastava, S.A. Agnihotry, M. Deepa, Thin Solid Films, **515**, 1419 (2006).
[21] A.M. Torres-Huerta, M.A. Dominguez-Crespo, E. Ramirez-Meneses, J.R. Vargas-Garcia, Appl. Surf. Sci. **255**, 4792 (2009).
[22] S.S. Lin, J.L. Huang, D.F. Lii, Mater. Chem. Phys. **90**, 22 (2005).
[23] A. Enesca , A. Duta ,J. Schoonman, Thin Solid Films **515**, 6371 (2007).
[24] S.M. Yong, T. Nikolay, B. T. Ahn, D. K. Kim, J. Alloys Compnds. **547**, 113 (2013).